Synthesis, Structure, and Solution NMR Studies of Cyanide−Copper(II) and Cyanide-Bridged Iron(III)−Copper(II) Complexes

Daniele M. Corsi,[†,§] Narasimha N. Murthy,[†,||] Victor G. Young, Jr.,[‡] and and Kenneth D. Karlin*[,†]

The Department of Chemistry, The Johns Hopkins University, Charles and 34th Streets, Baltimore, Maryland 21218, and The X-ray Crystallographic Laboratory, Department of Chemistry, The University of Minnesota, 207 Pleasant St. S.E., Minneapolis, Minnesota 55455

Received September 10, 1998

A range of small molecules, such as cyanide, are known to bind and/or inhibit the active site of the heme-copper oxidase enzymes. As such, model studies are aimed at elucidating ligand binding modes and their subsequent impact on spectroscopic properties of derived complexes. We describe here the isolation and characterization of two compounds containing the Fe−CN−Cu moiety, $[(py)(F_8\text{-TPP})Fe^{III}\text{-CN-}Cu^{II}(TMPA)]^{2+}$ (**5**) and $[(F_8\text{-TPP})Fe^{III}\text{-}(CN)_2\text{-}\{Cu^{II}(TMPA)\}_2]^{3+}$ (**6**) [py = pyridine, TMPA = tris(2-pyridylmethyl)amine, and $(F_8$-TPP) = tetrakis-(2,6-difluorophenyl)porphyrinate(2−)]. $[Cu^{II}(TMPA)(CH_3CN)](ClO_4)_2$ and $[(py)(F_8\text{-TPP})Fe^{III}(CN)]$ (**3**) react to yield **5**, while **6** is formed by combination of $[Cu^{II}(TMPA)(CN)]PF_6$ (**2**-(PF_6)) and $[(F_8\text{-TPP})Fe^{III}(PF_6)]$ (**4**). Complex **2**-(PF_6) crystallizes in the orthorhombic space group *Iba*2 with $a = 17.2269(5)$ Å, $b = 17.3143(4)$ Å, and $c = 14.4971(4)$ Å, $Z = 8$, complex (**5**-$(Sb/P)F_6)_{1.5}(ClO_4)_{0.5}$ was obtained in the orthorhombic space group *P*222 with $a = 17.9541(2)$ Å, $b = 20.5359(1)$ Å, and $c = 21.2023(2)$ Å, $Z = 4$, and **6**-$(PF_6)_3$ crystallized in the monoclinic space group $P2_1/c$ with $a = 15.318(4)$ Å, $b = 33.921(2)$ Å, and $c = 19.649(6)$ Å, $\beta = 109.69(2)°$, and $Z = 4$. Compound **5** possesses a low-spin iron(III) center, bridged via cyanide to copper. The iron−cyanide vector deviates slightly from linearity (174.6(5)°). The copper(II) ion is five-coordinated by the TMPA N-donor atoms and the cyanide carbon atom. The Cu(TMPA) moiety is bent with an angle of 163.8(5)° around the cyanide−copper vector. Compound **6** possesses a low-spin iron(III) atom axially coordinated by two cyanide ligands capped on either side by trigonally coordinated [Cu(TMPA)] moieties. The [Cu(1)(TMPA)] unit is twisted somewhat (∠Cu1−N≡C = 168°), whereas the [Cu(2)(TMPA)] unit is coordinated in a nearly linear fashion with respect to the cyanide−iron vector (∠Cu2−N≡C4 = 175°). ^{1}H and ^{2}H NMR spectroscopy on **5** and **6** confirmed the low-spin nature of these iron complexes (pyrrole resonance found at −11.1 and −8 ppm, respectively). The NMR data as well as observed solution magnetic moment ($\mu_B = 2.7$ for **5**; $\mu_B = 3.4$ for **6**) suggest ferromagnetic coupling between the paramagnetic metal ions. This gives rise to an enhancement of the electronic relaxation rate for Cu(II) in both **5** and **6** allowing for the observation of the sharp and downfield shifted TMPA ligand proton signals.

Introduction

The synthesis of porphyrin-containing multimetal arrays is a continuing subject of study. Targeted preparation and isolation of different compounds may allow for a comparison with one of Nature's most enigmatic metalloproteins, cytochrome *c* oxidase (C*c*O), the terminal protein in the respiratory chain.[1] The enzyme functions by coupling the reduction of dioxygen to water with "pumping" of protons across the mitochondrial membrane. This action sets up a membrane potential used to drive ATP synthesis.

A corpus of information has been published on various aspects of the structure and function of C*c*O. A most important recent advance occurred in 1995 when two groups independently reported X-ray crystal structures of *Paracoccus denitrificans* and bovine heart cytochrome *c* oxidase.[2] These reports confirmed previously held notions concerning the heme-copper active site responsible for the O_2-reduction chemistry. The resting state Fe(III) heme a_3 moiety is axially coordinated by a single histidine residue. The Cu_B ion, ligated by three histidines, resides at a distance of ∼4.5 Å from this iron.[2c,d]

Despite the structural advances, many questions remain unanswered. There has been a continued interest in the oxidized, "resting" state of the enzyme, since it is readily accessible and amenable to inquiry by various spectroscopic or physical

* To whom correspondence should be addressed. E-mail: karlin@jhu.edu.
† Johns Hopkins University.
‡ University of Minnesota.
§ Current address: Laboratory of Organic Chemistry and Catalysis, Delft University of Technology, Julianalaan 136, 2628 BL Delft, The Netherlands.
|| Current address: Department of Chemistry, IIT Madras, Madras 600036, India.

(1) (a) Malmström, B. G. *Acc. Chem. Res*. **1993**, *26*, 332−338. (b) Babcock, G. T.; Wikström, M. *Nature* **1992**, *356*, 301−309. (c) Malmstrom, B. G. *Chem. Rev*. **1990**, *90*, 1247−1260. (d) Chan, S. I.; Li, P. M. *Biochemistry*. **1990**, *29*, 1−12. (e) Calhoun, M. W.; Thomas, J. W.; Gennis, R. B. *Trends. Biochem. Sci*. **1994**, *19*, 325. (f) Ferguson-Miller, S.; Babcock, G. T. *Chem. Rev.* **1996**, *96*, 2889−2907.

(2) (a) Iwata, S.; Ostenmeier, C.; Ludwig, B.; Michel, H. *Nature* **1995**, *376*, 660−669. (b) Tsukihara, T.; Aoyama, H.; Yamashita, E.; Tomizaki, T.; Yamaguchi, H.; Shinzawa-Itoh, K.; Nakashima, R.; Yaono, R.; Yoshikawa, S. *Science* **1995**, *269*, 1069−1074. (c) Ostermeier, C.; Harrenga, A.; Ermler, U.; Michel, H. *Proc. Natl. Acad. Sci. U.S.A.* **1997**, *94*, 10547−10553. (d) Yoshikawa, S.; Shinzawa-Itoh, K.; Nakashima, R.; Yaono, R.; Yamashita, E.; Inoue, N.; Yao, M.; Fei, M. J.; Peters Libeu, C.; Mizushima, T.; Yamaguchi, H.; Tomizaki, T.; Tsukihara, T. *Science* **1998**, *280*, 1723−1729.

10.1021/ic981091s CCC: $18.00
Published on Web 03/08/1999

methods; it may also represent one of the turnover states in the functioning enzyme reaction cycle. Resonance Raman and Mössbauer spectroscopies implicate a high-spin iron(III) ($S = {}^5/_2$) for the heme a_3 along with an $S = {}^1/_2$ Cu(II) Cu_B ion.[3] Magnetic susceptibility data have been interpreted as an Fe−Cu entity having an $S = 2$ spin state which is EPR silent.[4,5] These observations have been previously explained by the presence of a [Fe^{III}-X-Cu^{II}] unit, in which X represents a bridging ligand that modulates antiferromagnetic coupling. Naturally occurring X groups proposed include chloride (Cl^-), sulfide (S^{2-}), imidazolate, phenoxide (PhO^-), oxide (O^{2-}), and hydroxide (OH^-).[6,7] Another question concerns the magnitude of the exchange coupling between the two metals. In a recent detailed study simulating dual-mode EPR spectra,[8] the authors conclude that the two metals actually are only *weakly* interacting and this coupling is not significantly influenced by a ligand between them, i.e., fluoride, formate, or azide. The original X-ray structure reports[2a,b] did not detect a bridging unit between Cu_B and heme a_3; however, the more recent refined structures indicate a continuous electron density between the metal ions.[2c,d]

The design, isolation, and characterization of ligand-bound and bridged heme-copper model compounds may provide a necessary element in the completion of an accurate picture of C*c*O. Various groups have contributed significantly, by synthesizing and characterizing bridged heme-Cu multinuclear arrays.[9−14] Included are small-molecule analogues [(P)Fe^{III}-X-Cu^{II}(L)] (P = porphyrinate, L = copper-ligand), where X = O^{2-} (oxo) and OH^-.[13,14] Among these from our laboratories is [(F_8-TPP)Fe^{III}-O-Cu^{II}(TMPA)]$^+$ (see diagram) [F_8-TPP = tetrakis(2,6-difluorophenyl)porphyrinate(2−); TMPA = tris(2-pyridylmethyl)amine].[14] The μ-oxo complex is notably basic

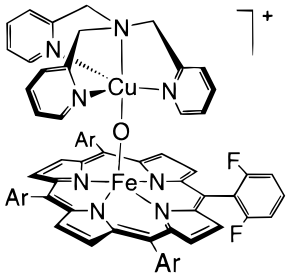

[(F_8-TPP)Fe-O-Cu(TMPA)]$^+$

and may be reversibly protonated to the hydroxo-bridged species [(F_8-TPP)Fe^{III}-OH-Cu^{II}(TMPA)]$^{2+}$.[14b] Structural comparisons and magnetic characteristics (antiferromagnetic coupling of spins) indicate that such hydroxo-bridged analogues are possible candidates for resting state enzyme mimics.[7b,14b]

As described, studies carried out with oxidized metal-bound exogeneous ligands such as azide (N^{3-}), cyanide (CN^-), thiocyanide (SCN^-), formate (HCO_2^-), and hydrogen peroxide (H_2O_2) are of interest.[7b,8,15] Such adducts serve as site probes amenable to study by spectroscopic techniques including FT-IR, UV−vis, EPR, MCD, and Mössbauer spectroscopies as well as magnetic measurements. Also of great importance is the lethal toxicity of cyanide as it has been linked to the irreversible binding at the dinuclear site and consequent inhibition of C*c*O.[1,16] Upon binding to the oxidized enzyme, cyanide causes the Fe(III) heme a_3 to revert from high spin ($S = {}^5/_2$) to low spin ($S = {}^1/_2$) and alters the various spectroscopic properties (vide supra) associated with the dinuclear center. A notable consequence is the switch to ferromagnetic exchange coupling between the two spins as the cyanide ligand bridges the two metals.[19] Thus, synthetic models of the μ-CN^- heme-copper moieties have also received considerable attention.[9,12]

There is an additional fundamental significance of this work related to the understanding of magnetic interactions in hetero-

(3) (a) Kent, T. A.; Young, L. J.; Palmer, G.; Fee, J. A.; Munck, E. *J. Biol. Chem.* **1983**, *258*, 8543. (b) Babcock, G. T.; Callahan, P. M.; Ondrial, M. R.; Selmeen, I. *Biochemistry* **1981**, *20*, 959.
(4) (a) Day, E. P.; Peterson, J.; Sendova, M. S.; Schoonover, J.; Palmer, G. *Biochemistry* **1993**, *32*, 7855−7860. (b) Barnes, Z. K.; Babcock, G. T.; Dye, J. L. *Biochemistry* **1991**, *30*, 7597−7603.
(5) (a) Brudvig, G. W.; Moore, R. H.; Chan, S. I. *J. Magn. Reson.* **1986**, *67*, 189. (b) Hartzell, C. R.; Hansen, R. E.; Beinert, H. *Proc. Natl. Acad. U.S.A.* **1973**, *70*, 2477.
(6) Kitajima, N. *Adv. Inorg. Chem.* **1992**, *39*, 1−77.
(7) (a) Powers, L.; Lauraeus, M.; Reddy, K. S.; Chance, B.; Wikström, M. *Biochim. Biophys. Acta* **1994**, *1183*, 504−512. (b) Fann, Y. C.; Ahmad, I.; Blackburn, N. J.; Boswell, J. S.; Verkhovskaya, M. L.; Hoffman, B. M.; Wikström, M. *Biochemistry* **1995**, *34*, 10245−10255.
(8) Oganesyan, V. S.; Butler, C. S.; Watmough, N. J.; Greenwood, C.; Thomson, A. J.; Cheesmen, M. R. *J. Am. Chem. Soc.* **1998**, *120*, 4232−4233.
(9) Gunter, M. J.; Mander, L. N.; Murray, K. S.; Clark, P. E. *J. Am. Chem. Soc.* **1981**, *103*, 6784−6787. (b) Gunter, M. J.; Berry, K. J.; Murray, K. S. *J. Am. Chem. Soc.* **1984**, 106, 4227−4235. (c) Gunter, M. J.; Mander, L. N.; Murray, K. S. *J. Chem. Soc., Chem. Commun.* **1981**, 799−801. (d) Gunter, M. J.; Turner, P. *Coord. Chem. Rev.* **1991**, *108*, 115−161.
(10) (a) Serr, B. R.; Headford, C. E. L.; Anderson, O. P.; Elliot, C. M.; Spartalian, K.; Fainzilberg, V. E.; Hatfield, W. E.; Rohrs, B. R.; Eaton, G. E. *Inorg. Chem.* **1992**, *31*, 5450−5465. (b) Elliott, C. M.; Jain, N. C.; Cranmer, B. K.; Hamburg, A. W. *Inorg. Chem.* **1987**, *26*, 3655−3659.
(11) (a) Casella, L.; Monzani, E.; Gullotti, M.; Gliubich, F.; De Gioia, L. *J. Chem. Soc., Dalton Trans.* **1994**, 3203−3210. (b) Casella, L.; Gullotti, M.; *Bioinorganic Chemistry of Copper*; Karlin, K. D., Tyeklár, Z., Eds.; Chapman & Hall: New York, 1993; pp 292−305.
(12) For μ-CN^- complexes see: (a) Lee, S. C.; Scott, M. J.; Kauffmann, K.; Münck, E.; Holm, R. H. *J. Am. Chem. Soc.* **1994**, *116*, 401−402. (b) Scott, M. J.; Holm, R. H. *J. Am. Chem. Soc.* **1994**, *116*, 11357−11367. (c) Scott, M. J.; Lee, S. C.; Holm, R. H. *Inorg. Chem.* **1994**, *33*, 4651−4662. (d) Holm, R. H. *Pure Appl. Chem.* **1995**, *67*, 217−224. (e) Gardner, M. T.; Deinum, G.; Kim, Y.; Babcock, G. T.; Scott, M. J.; Holm, R. H. *Inorg. Chem.* **1996**, *35*, 6878−6884. (f) Zhang, H. H.; Filipponi, A.; Di Cicco, A.; Scott, M. J.; Holm, R. H.; Hedman, B.; Hodgson, K. O. *J. Am. Chem. Soc.* **1997**, *119*, 2470−2478. (g) Lim, B. S.; Holm, R. H. *Inorg. Chem.* **1998**, *37*, 4898−4908.
(13) For μ-O^{2-}, μ-OH^-, μ-F^-, and μ-RCO_2^- compounds, see: (a) Lee, S. C.; Holm, R. H. *J. Am. Chem. Soc.* **1993**, *115*, 5833−5834. (b) Lee, S. C.; Holm, R. H. *J. Am. Chem. Soc.* **1993**, *115*, 11789−11798. (c) Scott, M. J.; Zhang, H. H.; Lee, S. C.; Hedman, B.; Hodgson, K. O.; Holm, R. H. *J. Am. Chem. Soc.* **1995**, *117*, 568−569. (d) Scott, M. J.; Goddard, C. A.; Holm, R. H. *Inorg. Chem.* **1996**, *35*, 2558−2567. (e) Zhang, H. H.; Filipponi, A.; Di Cicco, A.; Lee, S. C.; Scott, M. J.; Holm, R. H.; Hedman, B.; Hodgson, K. O. *Inorg. Chem.* **1996**, *35*, 4819−4828.
(14) (a) Karlin, K. D.; Nanthakumar, A.; Fox, S.; Murthy, N. N.; Ravi, N.; Huynh, B. H.; Orosz, R. D.; Day, E. P. *J. Am. Chem. Soc.* **1994**, *116*, 4753−4763. (b) Fox, S.; Nanthakumar, A.; Wikström, M.; Karlin, K. D.; Blackburn, N. J. *J. Am. Chem. Soc.* **1996**, *118*, 24−34.
(15) (a) Tsubaki, M. *Biochemistry* **1993**, *32*, 174. (b) Tsubaki, M.; Mogi, T.; Anraku, Y.; Hori, H. *Biochemistry* **1993**, *32*, 6065−6072. (c) Li, W.; Palmer, G. *Biochemistry* **1993**, *32*, 1833. (d) Watmough, N. J.; Cheesman, M. R.; Gennis, R. B.; Greenwood, C.; Thomson, A. J. *FEBS Lett.* **1993**, *319*, 151. (e) Ingledew, W. J.; Horrocks, J.; Salerno, J. C. *Eur. J. Biochem.* **1993**, *212*, 657. (f) Yoshikawa, S.; Caughey, W. S. *J. Biol. Chem.* **1992**, *267*, 9757. (g) Surerus, K. K.; Oertling, W. A.; Fan, C.; Burgiel, R. J.; Einarsdottir, O.; Antholine, W. E.; Dyer, R. B.; Hoffman, B. M.; Woodruff, W. H.; Fee, J. A. *Proc. Natl. Acad. Sci. U.S.A.* **1992**, *89*, 3195. (h) Weng, L.; Baker, G. M. *Biochemistry* **1991**, *30*, 5727−5733.
(16) Labianca, D. A. *J. Chem. Educ.* **1979**, *56*, 788.
(17) Nanthakumar, A.; Fox, S.; Murthy, N. N.; Karlin, K. D. *J. Am. Chem. Soc.* **1997**, *119*, 3898−3906.
(18) (a) Bertini, I.; Luchinat, C. In *Physical Methods for Chemists*, 2nd ed.; Drago, R. S., Ed.; Harcourt Brace Jovanovich: Orlando, FL, 1992; pp 500−556. (b) Luchinat, C.; Ciurli, S. In *Biological Magnetic Resonance, Vol. 12, NMR of Paramagnetic Molecules*; Berliner, L. J., Reuben, J., Eds.; Plenum Press: New York, 1993; pp 357−420. (c) Bertini, I.; Luchinat, C. *NMR of Paramagnetic Substances*; Elsevier: Amsterdam, 1996. (d) Clementi, V.; Luchinat, C. *Acc. Chem. Res.* **1998**, *31*, 351−361.
(19) Thomson, A. J.; Eglinton, D. G.; Hill, B. C.; Greenwood, C. *Biochem. J.* **1982**, *207*, 167−170.

metallic complexes. There exist few examples of *ferromagnetically* coupled heteronuclear $Fe^{III}-Cu^{II}$ systems.[9b,12a,20] In representative compounds, magnetic coupling is facilitated through various bridging ligands including cyanide,[9b,12a] phenolate,[20a] and imidazolate.[20b]

In this report, we detail our own efforts in the synthesis, structural descriptions, and spectroscopic characterizations of new μ-cyano complexes, $[(py)(F_8\text{-TPP})Fe^{III}\text{-CN-}Cu^{II}(TMPA)]^{2+}$ (**5**) (py = pyridine), and the trinuclear species, $[(F_8\text{-TPP})Fe^{III}\text{-}(CN)_2\text{-}\{Cu^{II}(TMPA)\}_2]^{3+}$ (**6**). Paramagnetically shifted NMR properties, in particular, are presented against the background of previously detailed NMR studies on $[(F_8\text{-TPP})Fe^{III}\text{-O(H)-}Cu^{II}(TMPA)]^{+/(2+)}$.[17] Although ^{1}H NMR spectra of mononuclear Cu(II) complexes are normally not observed, magnetic coupling to a second, faster relaxing nucleus (here Fe(III)) provides a means for attenuation of the nuclear relaxation rate, resulting in sharper NMR signals,[17,18,21] observed here. The present case provides an example of a feromagnetically coupled $Fe^{III}-Cu^{II}$ complex and demonstrates the magnetically induced isotropic shifts resulting for such iron−copper coupled systems.

Experimental Section

Warning. Although we have experienced no difficulties with the perchlorate complexes described, *these should be regarded as potentially explosive and handled accordingly.*[22]

Synthetic Methods. F_8-$TPPH_2$, [(F_8-TPP)FeCl], (F_8-TPP)Fe_2O, and their pyrrole deuterated varieties were synthesized as described previously.[14a] The ligand TMPA,[23] $[Cu^{II}(TMPA)(CH_3CN)](ClO_4)_2$,[14b] methylene deuterated TMPA,[17] and the methyl-substituted series (*n*-Me)$_3$-TMPA (n = 3, 4, 5)[17] were prepared following the literature procedures. Other chemicals were obtained from commercial sources. D_2O (99.9%) was purchased from Aldrich Chemical Co. Diethyl ether and THF were predried over KOH, and filtered and distilled over sodium/benzophenone under an argon atmosphere. Methanol was distilled from $Mg(OMe)_2$, acetone from B_2O_3, acetonitrile from CaH_2, heptane and toluene from Na(s), all under argon atmospheres. Using separatory funnel treatments, dichloromethane was exposed to concentrated H_2SO_4, shaken with Na_2CO_3 solution, and then washed with distilled water. The separated CH_2Cl_2 layer was dried over $MgSO_4$, filtered, and predried over CaH_2 before a final distillation over CaH_2 under an argon atmosphere. Metalation of the various porphyrins with $FeCl_2$ (Fluka) was carried out under an argon atmosphere using standard Schlenk techniques.

Physical Methods. Elemental analyses were preformed by Desert Analytics (Tucson, AZ) and National Chemical Consulting Inc. (Tenafly, NJ). ^{1}H and ^{2}H NMR spectra were obtained at 300 and 46 MHz, respectively, on a Bruker AMX-300 instrument. Chemicals shifts are reported as δ values, downfield from an internal standard (Me_4Si) or the residual solvent proton peak (for ^{1}H NMR). All ^{2}H NMR spectra were run in $CHCl_3$ solvent with 2 μL of $CDCl_3$ added as an internal reference. ^{19}F NMR spectra were recorded at 376 MHz on a Varian XL-400 instrument. Infrared spectra were obtained on a Mattson Galaxy 4030 FT-IR spectrometer. Solid samples were run as KBr pellets or as Nujol mulls. UV−vis spectra were recorded on a Shimadzu UV 160 spectrometer. Solution magnetic moment measurements were obtained using the Evans method.[24] To this end, samples with known concentration were made up in $CDCl_3$ solution. From the downfield shift of the TMS signal with respect to that from the capillary reference tube, the paramagnetic susceptibility χ'_m was calculated using the following formula: $\chi'_m \cong (-3/4\pi)(\Delta\nu/\nu)(1000/c) + (\chi_0 M_w) - \chi_D$,[25] where $\Delta\nu$ is the difference in shift of the reference signal in Hz, ν is the spectrometer frequency, c is the concentration of the complex in moles per liter, χ_0 is the solvent susceptibility, M_w is the molecular weight of the complex and χ_D is the diamagnetic contribution to the susceptibility. The latter was calculated using tabulated Pascal's constants.[26] The magnetic moment μ_{eff} is the derived from the following formula: $\mu_{eff} = 2.84\sqrt{(\chi'_m T)}$.

$[Cu^{II}(TMPA)Cl]PF_6$ (1-(PF_6)). This complex was prepared using a modification of the procedure described earlier,[23b,27] giving material with the spectroscopic properties previously reported.[27] A solution of $CuCl_2\cdot 2H_2O$ (0.685 g, 4.00 mmol) in 40 mL of CH_3OH was added to a stirring solution of TMPA (1.166 g, 4.00 mmol) in 40 mL of CH_3OH. The mixture was stirred for 45 min, whereupon a clear blue-green solution formed. A solution of $NaPF_6$ (3.565 g. 20.4 mmol) in 40 mL of CH_3OH was added to the reaction mixture, giving a change in color to light blue. The solid product obtained by precipitation with diethyl ether was redissolved in CH_2Cl_2 (25 mL), filtered, and precipitated with diethyl ether (100 mL). This procedure was repeated, yielding 1.80 g (84%) of light blue-green microcrystalline material. A final recrystallization from hot CH_3OH gave large crystalline needles. Anal. Calcd for $C_{18}H_{18}ClCuF_6N_4P$: C, 40.46; H, 3.40; N, 10.49. Found: C, 40.28; H, 3.39; N, 10.03. IR (Nujol, cm^{-1}): ca. 2900 (vs, C−H), 1609 (s, C═C), 1441 (vs), 1375 (m), 1310 (m), 1265 (m), 1161 (m), 1098 (m), 1055 (m), 1022 (m), 959 (m), ca. 40 (vs, br, PF_6^-), 768 (vs), 650 (w), 557 (vs). UV−vis (CH_3CN; λ_{max}, nm): 301, 960.

$[Cu^{II}(TMPA)(CN)]PF_6$ (2-(PF_6)). To a stirring solution of $[Cu^{II}(TMPA)Cl]PF_6$ (**1**, 0.539 g, 1.00 mmol) in 15 mL CH_2Cl_2 was added a methanolic solution (15 mL) of NaCN (0.058 g, 1.10 mmol). A color change from blue-green to intense royal blue was observed upon addition although stirring was continued for 1 h. The resulting solution was layered with 200 mL of diethyl ether and placed at 8 °C for several days. A powder-blue precipitate was collected, redissolved in CH_2Cl_2 (30 mL), filtered and reprecipitated with Et_2O (200 mL) yielding 0.467 g (89%) of a powder blue solid. A final recrystallization from hot CH_3OH gave large crystalline needles. Anal. Calcd for $C_{19}H_{18}N_5F_6PCu\cdot CH_3OH$: C, 43.16; H, 3.99; N, 12.59. Found: C, 43.14; H, 3.47; N, 12.76. IR (KBr, cm^{-1}): ca. 2900 (vs, C−H), 2147 (w, CN^-), 1607 (s, C═C), 1411 (s), 1375 (m), 1308 (m), 1161 (m), 1022(s), ca. 830 (vs, br, PF_6^-), 768 (s), 650 (m), 557 (s). UV−vis (CH_3CN, λ_{max}, nm): 293, 817.

$[(py)(F_8\text{-TPP})Fe^{III}(CN)]$ (3). The preparation of similar compounds using different porphyrins has been reported previously.[12a,c,28] Under an argon atmosphere, 0.323 g (0.197 mmol) of $[(F_8\text{-TPP})Fe]_2O$ was dissolved in 12 mL of a dry CH_2Cl_2/pyridine (9:1, v/v) solution. A 10% excess of trimethylsilyl cyanide was added by syringe, and stirring was continued under argon for 24 h producing a brilliant scarlet solution. The reaction mixture was concentrated to dryness under reduced pressure leaving a crude residue which was recrystallized from equal volumes of CH_2Cl_2/heptane (12 mL) yielding 0.322 g (89%) of metallic, violet microcrystals. Anal. Calcd for $C_{50}H_{25}N_6F_8Fe$: C, 65.45; H, 2.75; N, 9.16. Found: C, 65.23; H, 2.85; N, 8.79. ^{1}H NMR (CD_2Cl_2): δ18.3 ppm (pyridine), 10.1 (pyridine), 6.3, 5.7, 1.6 (pyridine), −19.6 (pyrrole). IR (KBr, cm^{-1}): 1624 (s), 1464 (s), 1236 (m), 999 (vs), 783 (m). UV−vis (CH_2Cl_2; λ_{max}, nm (ϵ, M^{-1} cm^{-1})): 326 (23 000), 416 (Soret, 96 000), 554 (5400).

$[(F_8\text{-TPP})Fe^{III}(PF_6)]$ (4). This synthesis is a modified version of that reported earlier for tetraphenylporphyrin.[29] In an inert atmosphere box, [(F_8-TPP)FeCl] (0.30 g, 0.354 mmol) and $AgPF_6$ (0.12 g, 0.460

(20) (a) Juarez-Garcia, C.; Hendrich, M. P.; Holman, T. R.; Que, L.; Münck, E. *J. Am. Chem. Soc*. **1991**, *113*, 518−525. (b) Gupta, G. P.; Lang, G.; Koch, C. A.; Wang, B.; Scheidt, W. R.; Reed, C. A. *Inorg. Chem*. **1990**, *29*, 4234−4239.
(21) Murthy, N. N.; Karlin, K. D.; Bertini, I.; Luchinat, C. *J. Am. Chem. Soc*. **1997**, *119*, 2156−2162.
(22) Wolsey, W. C. *J. Chem. Educ*. **1973**, *50*, A335.
(23) (a) Tyeklár, Z.; Jacobson, R. R.; Wei, N.; Murthy, N. N.; Zubieta, J.; Karlin, K. D. *J. Am. Chem. Soc*. **1993**, *115*, 2677−2689. (b) Jacobson, R. R. Ph.D. Dissertation, State University of New York at Albany, 1989.
(24) (a) Evans, D. F. *J. Chem. Soc*. **1959**, 2003. (b) Live, D. H.; Chan, S. I. *Anal. Chem*. **1970**, *42*, 791−792.
(25) Sur, S. K. *J. Magn. Reson*. **1973**, *12*, 286.
(26) Carlin, R. L. *Magnetochemistry*; Springer-Verlag: New York, 1986.
(27) Karlin, K. D.; Hayes, J. C.; Juen, S.; Hutchinson, J. P.; Zubieta, J. *Inorg. Chem*. **1982**, *21*, 4106−4108.
(28) (a) Uno, T.; Hatano, K.; Nishimura, Y. *Inorg. Chem*. **1988**, *27*, 3215. (b) Scheidt, W. R.; Hatano, K. *Acta Crystallogr*. **1991**, *C47*, 2201.
(29) Reed, C. A.; Mashiko, T.; Bentley, S. P.; Kastner, M. E.; Scheidt, W. R.; Spartalian, K.; Lang, G. *J. Am. Chem. Soc*. **1979**, *101*, 2948−2958.

mmol) were weighed and transferred to an airless flask equipped with a stir bar and ground glass stopper. The solid material was dissolved in 35 mL of freshly distilled THF and the solution was stirred at room temperature for 15 min to facilitate complete dissolution. The reaction mixture was then refluxed gently (65 °C) under Ar for 15 min followed by filtration to remove AgCl. The filtrate was layered with 150 mL of heptane and stored at 8 °C for several days. A solid purple product was filtered and dried in vacuo overnight, yielding 0.32 g (93%). ^{1}H NMR (CD_2Cl_2): δ 76.5 (v br, pyrrole), 13.4, 12.3 (*meta*-phenyl), 8.2 (*para*-phenyl). IR (Nujol, cm^{-1}): ca. 2900 (vs, C−H), 1624 (s), 1582 (m), 1464 (s), 1377 (m), 1275 (m), 1235 (m), 999 (vs), 843 (s, PF_6^-), 783 (m), 714 (m), 579 (m). UV−vis (CH_2Cl_2; λ_{max}, nm): 325, 409 (Soret).

Iron−Copper Bridged Complexes. [(py)(F_8-TPP)Fe^{III}-CN-Cu^{II}-(TMPA)](ClO$_4$)$_2$ (5-(ClO$_4$)$_2$). A 0.09 g (0.098 mmol) amount of [(py)-(F_8-TPP)Fe(CN)] was combined with 1 equiv of [Cu(TMPA)CH_3CN]-(ClO_4)$_2$ (0.058 g), and the solid mixture was stirred under vacuum and purged with argon prior to the addition of 4 mL of acetone. The resulting bright red solution was layered with excess diethyl ether (15 mL) and placed overnight at 8 °C, producing a violet microcrystalline solid. Final recrystallization from CH_2Cl_2/toluene (12 mL) afforded 0.128 g (89%) of **5**. Anal. Calcd for $C_{68}H_{43}N_{10}O_8F_8Cl_2FeCu\cdot 4H_2O$ (presence of H_2O verified by NMR spectroscopy): C, 52.95; H, 3.33; N, 9.08. Found: C, 52.75; H, 2.94; N, 9.05. ^{1}H NMR (CD_2Cl_2): δ 167.9 ppm (TMPA methylene), 74.3 (TMPA 6-pyridyl H), 33.2 (TMPA 3-pyridyl H), 32.3 (TMPA 5-pyridyl H), 10.6 (TMPA 4-pyridyl H), 9.1 (pyridine), 7.9, 7.7 (F_8-TPP *meta*-phenyl), 7.1 (F_8-TPP *para*-phenyl), 1.26 (H_2O), −11.1 (pyrrole), −15.5 (pyridine). IR (KBr, cm^{-1}): 2170 (w, CN^-), 1624 (s), 1611 (s), 1464 (s), 1082 (s, ClO_4^-), 999 (vs), 763 (m). UV−vis (CH_2Cl_2; λ_{max}, nm (ϵ, M^{-1} cm^{-1})): 256 (26 500), 330 (21 550), 414 (107 000), 539 (6700). Magnetic moment (solution in $CDCl_3$, room temperature) $\mu_{eff} = 2.7\ \mu_B$.

[(F_8-TPP)Fe^{III}-(CN)$_2$-{Cu^{II}(TMPA)}$_2$](PF$_6$)$_3$ (6-(PF$_6$)$_3$). In the inert atmosphere box, the following solid materials were transferred to a Schlenk flask (200 mL): 0.228 g (0.238 mmol) of [Fe(F_8-TPP)(PF_6)] (**4**) and 2 equiv of [Cu(TMPA)CN]PF_6 (**2**, 0.250 g, 0.476 mmol). Then, 20 mL of dry CH_2Cl_2 was used to dissolve the solid mixture. The resulting reddish-brown solution was stirred under argon for 1 h followed by filtration. The filtrate was layered with 30 mL heptane and placed at −20 °C overnight, precipitating a large quantity of crude material which was collected and recrystallized from CH_2Cl_2/heptane (20 mL). Red-purple needles were dried in vacuo, yielding 0.451 g (94%) of product. Anal. Calcd for $C_{82}H_{56}N_{14}F_{26}P_3FeCu_2$: C, 49.07; H, 2.81; N, 9.77. Found: C, 49.19; H, 3.0; N, 9.63. ^{1}H NMR (CD_2Cl_2): δ 157.5 ppm (TMPA methylene), 67.9 (TMPA 6-pyridyl H), 32.1 (TMPA 3-pyridyl H), 31.0 (TMPA 5-pyridyl H), 10.4, 10.2, 10.1 (TMPA 4-pyridyl H), 8.7, 8.5 (F_8-TPP *meta*-phenyl), 7.4 (F_8-TPP *para*-phenyl), −8.1 (pyrrole). IR (KBr, cm^{-1}): 2155 (w, CN^-), 1624 (s), 1611 (s), 1464 (s), 999 (vs), 845 (s, PF_6^-), 763 (m). UV−vis (CH_2Cl_2; λ_{max}, nm (ϵ, M^{-1} cm^{-1})): 332 (25 300), 421 (103 800), 543 (8600). Magnetic moment (solution in CD_2Cl_2, room temperature) $\mu_{eff} = 3.4\ \mu_B$.

X-ray Structure Determinations. Single crystals of **5** were obtained as a mixed counterion species [PF_6^-/SbF_6^-/ClO_4^-] formed by the metathetic reaction of the bisperchlorate **5** with excess sodium hexafluoroantimonate/sodium hexafluorophosphate in acetone followed by filtration and recrystallization from CH_2Cl_2 layered with cosolvent heptane. Crystals of **6**, suitable for X-ray analysis, were grown by slow diffusion of heptane into a CH_2Cl_2 solution of **6**. Single crystals of **2** were grown by recrystallization from hot methanol. Data for **5** and **2** were collected on a Siemens SMART system at 173 K, while **6** was on Rigaku AFC6S diffractometer, all three using Mo Kα (0.710 73 Å) radiation.

The space groups *P*222 for **5**, *Iba*2 for **2**, and $P2_1/c$ for **6** are determined based on the lack of systematic absences and intensity statistics.[30] All the three structures are solved by direct-methods, successive least-squares/difference Fourier cycles located all the non-hydrogen atoms, and they are refined with anisotropic displacement parameters unless stated otherwise. All hydrogen atoms are placed in ideal positions and refined as riding atoms with individual isotropic displacement parameters. A potpourri of anions and solvents were found for **5**: three-half (whole or partial) (Sb/P)F_6 anions, one-half ClO_4^-, and 1.5 dichloromethane plus 1.0 methanol solvents of crystallization are found per asymmetric unit. The admixture of both SbF_6^- and PF_6^- anions was found as a solid solution in all three sites. All sites were refined such that the Sb/P ratio summed to full occupancy. The overall Sb/P ratio is 0.65:0.35. Individual sites have refined ratios. All (Sb/P)−F bond lengths are intermediate in the range of 1.85 Å (Sb−F) and 1.58 Å (P−F). No attempt was made for the determination of two sets of fluorine positions, because of the solid solution effect. Among the three whole or partial (Sb/P)F_6 anions, the first, Sb(10)−F(16) is generally positioned and fully occupied. The others, Sb(20)−F(22) and Sb(30)−F(32) are located on independent 222 sites and each contributes $^1/_4$ charge. The remainder of anionic species are two interdependent ClO_4 anions on independent 222 sites that each contributes $^1/_4$ charge. The total count of anionic charge is −2 to balance the charge of the dication. The second perchlorate, Cl(50)−O(52), is disordered. The bond lengths, Cl−C, of the dichloromethane solvate vary greatly and may be influenced by some degree of disorder. For **2**, the PF_6 anion is equally split over two sites.

See Tables 1 and 2, Figures 1−3, and Supporting Information for further details of the X-ray structural determination of complexes **2**, **5**, and **6**.

Results and Discussion

Synthesis. The synthetic routes to the separate di- and trinuclear cyanide-bridged complexes are highlighted in Schemes 1 and 2. Enlisting these versatile materials as synthons, viz. [Cu^{II}(TMPA)Cl]$^+$ (**1**), [Cu^{II}(TMPA)(CH_3CN)]$^{2+}$ (**2**), [(F_8-TPP)-Fe]$_2$O, and [(F_8-TPP)Fe-Cl], enabled us to explore their cyanide chemistry. We have employed a self-assembly approach using these various copper and iron derivatives as precursors to the bridged systems. Two reaction pathways (eqs 1 and 2) were exploited to generate the different cyanide-bridged complexes:

$$[(py)(P)Fe^{III}(CN)] + [(L)Cu^{II}(CH_3CN)]^{2+} \rightarrow [(py)(P)Fe\text{-}(CN)\text{-}Cu(L)]^{2+} \quad (1)$$

$$(P)Fe^{III}\text{-}PF_6 + 2[(L)Cu^{II}(CN)]^+ \rightarrow [(P)Fe\text{-}\{(CN)\text{-}Cu(L)\}_2]^{3+} \quad (2)$$

Here, P represents the porphyrin (F_8-TPP) and L is the TMPA ligand on copper. In eq 1, the cyano group in [(py)(P)Fe^{III}(CN)] (**3**) provides the bridging ligand, leading to formation of the dinuclear-bridged assembly. The pyridine axial base fills the sixth coordination site on the iron, a characteristic feature of low-spin Fe(III) complexes.[31] Precedent for the eq 2 reaction pathway has been established,[12c] utilizing (P)Fe^{III}-PF_6 with its relatively noncoordinating ligand. Its reaction with the mononuclear cyanide copper complex allowed for the preparation of the trinuclear species.

Compound **3**, [(py)(F_8-TPP)Fe(CN)], was prepared from the μ-oxo dimer iron complex [(F_8-TPP)Fe]$_2$O, and trimethylsilyl cyanide in the presence of pyridine (Scheme 1), conditions previously explored by Holm et al.[12a] in their porphyrinate−Fe−CN−Cu chemistry.[12] Reaction of stoichiometric amounts of compounds **3** and [Cu^{II}(TMPA)(CH_3CN)](ClO_4)$_2$ in dry acetone under an argon atmosphere followed by precipitation with dry diethyl ether afforded the dinuclear complex [(py)-(F_8-TPP)Fe^{III}-CN-Cu^{II}(TMPA)](ClO_4)$_2$ (**5**-(ClO_4)$_2$). Single crystals of **5** were obtained as a mixed counterion species [PF_6^-/SbF_6^-/ClO_4^-] after reaction of the bis-perchlorate complex with

(30) *SHELXTL-Plus*, V5.0; Siemens Industrial Automation, Inc.: Madison, WI.

(31) Scheidt, W. R.; Reed, C. A. *Chem. Rev.* **1981**, *81*, 543−555.

Scheme 1

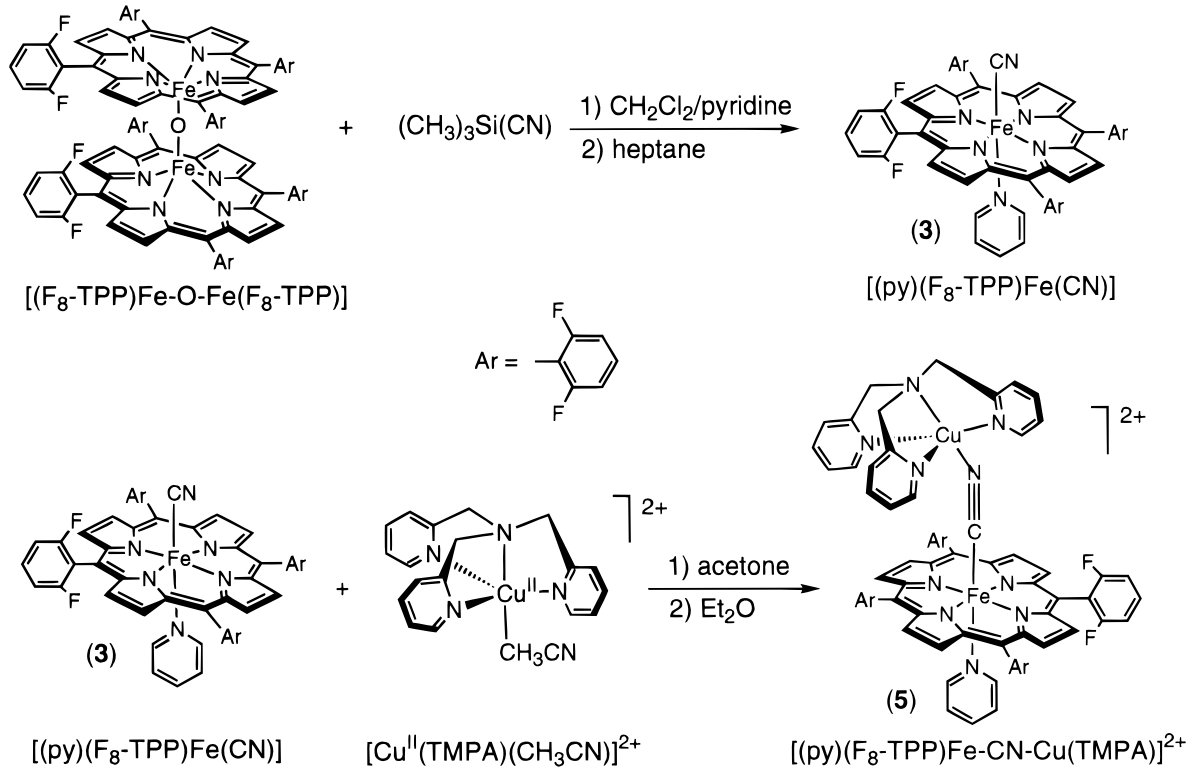

Scheme 2

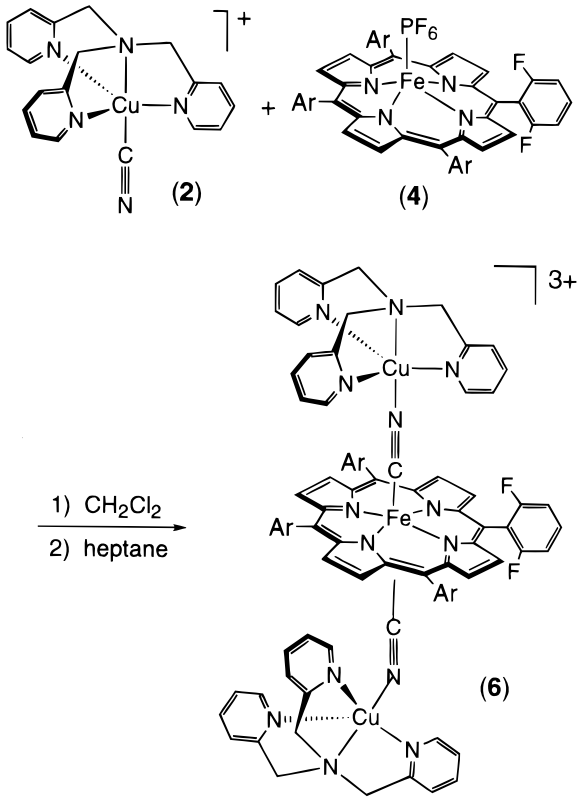

mixtures of excess sodium hexafluorophosphate and sodium hexafluoroantimonate.

Addition of a methanolic solution of NaCN to $[Cu^{II}(TMPA)Cl]PF_6$ (**1**-(PF_6)), dissolved in CH_2Cl_2, resulted in the formation of $[Cu^{II}(TMPA)(CN)]PF_6$ (**2**-(PF_6)). This sky-blue material is easily recrystallized from methanol yielding X-ray-quality single crystals. The existence of **2** as a Cu(II) complex is itself of some interest, since CN^- often reduces copper(II) to copper(I).[32] However, compared to related tripodal tetradentate ligands, TMPA is known to favor Cu(II) relative to Cu(I), based on electrochemical redox-potential comparisons.[27,33] When $[Cu^{II}(TMPA)(CN)]PF_6$ (**2-(PF_6)**) is combined in a 2:1 molar ratio with (F_8-TPP)Fe-PF_6 (obtained by reacting (F_8-TPP)Fe-Cl with $AgPF_6$), the trinuclear compound $[(F_8\text{-TPP})Fe^{III}\text{-}(CN)_2\text{-}\{Cu^{II}(TMPA)\}_2](PF_6)_3$ (**6-(PF_6)$_3$**) is obtained in high yield (94%) (eq 2 and Scheme 2). Although 5-coordinate monocyano Mn(III) porphyrins have been reported[34] and a monocyano Fe(III) porphyrin species has been investigated in solution[35] and suggested to exist in certain systems, we note that in the present case a monocyano-bridged (5-coordinate iron) binuclear Fe−Cu product was not observed even when a 1:1 reaction stoichiometry was imposed (i.e., in eq 2); rather, again the trinuclear product **6** was obtained in large quantities.

X-ray Structures. Experimental data for the X-ray structure data collection and analysis are given in Table 1. The molecular structure of the cationic portion of $[Cu^{II}(TMPA)(CN)](PF_6)$ (**2-(PF_6)**) is shown in Figure 1. Compound **2-(PF_6)** is a mononuclear pentacoordinate copper(II) species, with ligation to 4 N's from the TMPA ligand and a carbon from the cyanide ligand. The geometry around Cu(II) is best described as slightly distorted trigonal bipyramidal (TBP) with the pyridyl nitrogen atoms N(2), N(3), N(4) forming the equatorial plane and amine

(32) Hathaway, B. J. In *Comprehensive Coordination Chemistry*; Wilkinson, G., Ed.; Pergamon: New York, 1987; Vol. 5, pp 533−774.
(33) (a) Wei, N.; Murthy, N. N.; Karlin, K. D. *Inorg. Chem.* **1994**, 33, 6093−6100. (b) Zubieta, J.; Karlin, K. D.; Hayes, J. C. In *Copper Coordination Chemistry: Biochemical and Inorganic Perspectives*; Karlin, K. D., Zubieta, J., Eds.; Adenine Press: Albany, NY, 1983; pp 97−108.
(34) Scheidt, W. R.; Lee, Y. J.; Luangdilok, W.; Haller, K. J.; Anzai, K.; Hatano, K. *Inorg. Chem.* **1983**, *22*, 1516−1529.
(35) Wolowiec, S.; Latos-Grazynski, L. *Inorg. Chem.* **1994**, *33*, 3576−3586.

Table 1. Selected Crystal and Refinement Data for **2**, **5**, and **6**

	2	**5**	**6**
formula	$C_{19}H_{18}CuF_6N_5P$	$C_{70.25}H_{49.50}Cl_3CuF_{17}FeN_{10}O_3P_{0.55}Sb_{0.95}$	$C_{82}H_{56}N_{14}F_{26}P_3FeCu_2{\cdot}4CH_2Cl_2$
temp, K	173	173	183
M_w	524.89	1763.36	2346.99
cryst syst	orthorhombic	orthorhombic	monoclinic
space group	*Iba*2	*P*222	$P2_1/c$
a, Å	17.2269(5)	17.9541(2)	15.318(4)
b, Å	17.3143(4)	20.5359(1)	33.921(2)
c, Å	14.4971(4)	21.2023(2)	19.649(6)
α, deg	90	90	90
β, deg	90	90	109.69(2)
γ, deg	90	90	90
V, Å^3	4324.1(2)	7817.36(12)	9613(6)
F(000)	2120	3523	4708
Z	8	4	4
D_{calcd}, g/cm^3	1.613	1.498	1.622
abs coeff, cm^{-1}	1.152	0.985	9.62
no. of reflcns collcd	10 662	41 110	16 835
no. of indep reflcns ($I > 2\sigma(I)$)	3687	13782	6257 ($I > 3\sigma(I)$)
no. of refined params	309	972	1216
largest peak/hole, e Å^{-3}	0.496/−0.322	0.994/−0.606	2.31/−1.23
final *R* indices[a]	R1 = 0.0323	R1 = 0.0651	R1 = 0.094
	wR2 = 0.0806	wR2 = 0.1626	wR2 = 0.096

[a] $R1 = \sum||F_o|-|F_c||/\sum|F_o|$, $wR2 = [\sum[w(F_o^2 - F_c^2)^2]/\sum[w(F_o^2)^2)]]^{1/2}$, where $w = q/s^2(F_o^2) + (ap)^2 + bp$. $GOOF = S = [\sum[w(F_o^2 - F_c^2)^2]/(n - p)^2$.

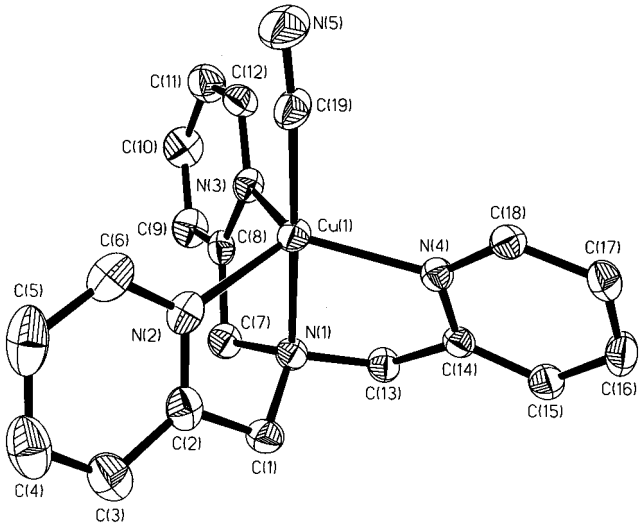

Figure 1. ORTEP view of the cation $[Cu^{II}(TMPA)(CN)]^+$ (**2**).

N(1) and cyanide carbon C(19) atoms in the axial positions. The τ value describing the geometry is 0.94 ($\tau = 1.00$ for a perfect TBP, 0.00 for square-pyramidal (SP));[36] TBP geometries are typical for complexes of TMPA, $[(TMPA)Cu^{II}\text{-}X]^{n+}$, X = Cl^-,[27] F^-,[37] CH_3CN,[17,23b] O_2^{2-},[23a] and even for a cobalt(II) analogue, $[(TMPA)Co(CH_3CN)]^{2+}$.[17] The Cu(II) ion is displaced from the basel plane toward C(19), by 0.32 Å. Selected bond distance and angle parameters for **2** are given in Table 2. The coordinated cyanide group is bent with ∠Cu(1)−C(19)−N(5) = 173.3(4)°, while the apex-to-apex vector formed by N(1)−Cu(1)−C(19) is essentially linear with an angle at 177.5(2)°. **2**-(PF_6) compares well in most aspects with the structure of $[Cu^{II}(Me_6tren)(CN)]ClO_4$ (Me_6tren = 2,2′,2″-tris(dimethylaminoethyl)amine),[12a] except for the small deviation from linearity (2.5°) of the Cu−cyanide vector as observed in the latter complex.

The cationic portion of the dinuclear complex $[(py)(F_8TPP)Fe^{III}(\mu\text{-}CN)Cu^{II}\text{-}(TMPA)](\{(Sb/P)F_6\}_{1.5}(ClO_4)_{0.5}{\cdot}1.5CH_2Cl_2{\cdot}$MeOH (**5**-X, X = $\{(Sb/P)F_6\}_{1.5}(ClO_4)_{0.5}$) is shown in Figure 2. The crystals contain 1.5 dichloromethane molecule and 1.0 methanol molecule of solvates per asymmetric unit and a potpourri of counteranions, $SbF_6/PF_6/ClO_4^-$, which were added to obtain X-ray diffraction quality crystals. The ferric ion is six-coordinate, ligated by the four pyrrole nitrogens (N(1) through N(4)), the pyridine nitrogen N(5), and the cyanide carbon C(50). The Fe(III) is in the plane of the pyrrole nitrogens; the Fe(1) vs (N(1), N(2), N(3), N(4)) displacement is 0.0121 Å (0.0102 dev.), as is usually observed for low-spin ferric porphyrins. The bonding parameters of the porphyrinate−iron(III) moiety are typical for low-spin iron(III)[31] and compare well with that of [(py)(TPP)Fe(CN)], reported by Scheidt *et. al.*[34] Thus the μ-CN^- ligand bridges to the copper ion such that the Fe(III)−porphyrin plane is capped by a $[(CN)Cu^{II}(TMPA)]^+$ moiety, with the axial pyridine ligand on the other side. The copper(II) ion is again five-coordinate with a slightly distorted trigonal bipyramidal geometry ($\tau = 0.90$) as in the mononuclear analogue $[Cu^{II}(TMPA)(CN)]^+$ (**2**) (vide supra). However, one important feature is the reversal of the binding mode of the cyano group; in **2**, the carbon of the cyanide ligand is bound to copper(II), as compared to nitrogen within the dinuclear complex **5**. Since the formal negative charge on cyanide is on the carbon atom, binding to the "harder" Fe(III) compared to Cu(II) is reasonable. The Fe(III)−cyanide ligand vector deviates slightly from linearity with ∠Fe(1)−C(50)−N(6) = 174.6(5)°. The TMPA amine−cupric−cyano nitrogen vector also approaches linearity, ∠N(10)−Cu(1)−N(6) = 177.4(2)°. The copper-(TMPA) moiety is bent with an angle of 163.8(5)° around C(50)−N(6)−Cu(1) (see also Scheme 1). This causes the TMPA moiety to sit partly slotted with two of its pyridine groups directed between phenyl groups of the porphyrin. All bond lengths (Table 2) for the copper−TMPA moiety in **5** are very similar to those observed for **2**. The bridging cyanide ligand with bond length, C(50)−N(6) = 1.141(8) Å, remains unchanged (from **2**) even with additional coordination to the iron-(III) center in $[(py)(F_8\text{-}TPP)Fe^{III}\text{-}CN\text{-}Cu^{II}(TMPA)]^{2+}$ (**5**).

The molecular structure of the trinuclear cationic portion of

(36) Addison, A. W.; Rao, T. N.; Reedijk, J.; van Rijn, J.; Verschoor, G. C. *J. Chem. Soc., Dalton Trans.* **1984**, 1349−1356.
(37) Jacobson, R. R.; Tyeklár, Z.; Karlin, K. D.; Zubieta, J. *Inorg. Chem.* **1991**, *30*, 2036−2040.

Table 2. Selected Bond Parameters for Compounds **2**, **5**, and **6**

interatomic distances (Å)		interatomic angles (deg)	
		$[Cu^{II}(TMPA)(CN)]PF_6$ (**2**-(PF_6))	
Cu(1)−C(19)	1.958(3)	N(1)−Cu(1)−C(19)	177.5(2)
Cu(1)−N(1)	2.046(2)	N(2)−Cu(1)−C(19)	99.9(2)
Cu(1)−N(2)	2.009(3)	N(3)−Cu(1)−C(19)	96.1(2)
Cu(1)−N(3)	2.075(3)	N(4)−Cu(1)−C(19)	100.6(1)
Cu(1)−N(4)	2.064(2)	N(2)−Cu(1)−N(3)	114.5(1)
C(19)−N(5)	1.142(4)	N(2)−Cu(1)−N(4)	117.6(1)
		N(3)−Cu(1)−N(4)	120.9(1)
		N−Cu(1)−N(rest), range	80.5(2)−81.5(1)
		Cu(1)−C(19)−N(5)	173.3(4)
		$[(Py)(F_8TPP)Fe^{III}$-(CN)-$Cu^{II}(TMPA)]$($\{(Sb/P)F_6\}_{1.5}(ClO_4)_{0.5}$·$1.5CH_2Cl_2$·MeOH (**5**-X)	
Fe(1)−C(50)	1.904(6)	Fe(1) Center	
Fe(1)−N (1−4), range	1.947(5)−1.980(5)	C(50)−Fe(1)−N(5)	177.0(2)
Fe(1)−N(5)	2.053(5)	C(50)−Fe(1)−N(1−4), range	88.5(2)−90.6(2)
Cu(1)−N(6)	1.945(6)	N(1)−Fe(1)−N(3)	179.2(2)
Cu(1)−N(1−4), range	2.024(6)−2.078(6)	N(2)−Fe(1)−N(4)	178.6(2)
C(50)−N(6)	1.141(8)	N(1,5)−Fe(1)−N(2,4), range	88.1(2)−93.2(2)
		N(6)−C(50)−Fe(1)	174.6(5)
		Cu(1) Center	
		N(6)−Cu(1)−N(10)	177.4(2)
		N(7)−Cu(1)−N(8)	114.5(3)
		N(7)−Cu(1)−N(9)	117.1(3)
		N(8)−Cu(1)−N(9)	123.2(3)
		N(6)−Cu(1)−N(7−9), range	96.3(2)−100.1(2)
		N(10)−Cu(1)−N(7−9), range	82.2(2)−82.5(2)
		$[(F_8$-TPP)Fe^{III}-$(CN)_2$-$\{Cu^{II}(TMPA)\}_2](PF_6)_3$·4 CH_2Cl_2 (**6**-$(PF_6)_3$·4 CH_2Cl_2)	
Fe(1)−Cu(1)	4.948(3)	Fe(1) Center	
Fe(1)−Cu(2)	5.027(3)	N−Fe(1)−N(trans)	177.8(6)−179.8(6)
Cu(1)−Cu(2)	9.955(4)	N−Fe(1)−N(cis), range	89.5(6)−90.4(6)
Fe(1)−C(45)	1.98(2)	C(45)−Fe(1)−N(1−4), range	86.6(6)−93.5(6)
Fe(1)−C(46)	1.98(2)	C(46)−Fe(1)−N(1−4), range	88.4(6)−92.1(6)
Fe(1)−N(1−4), range	1.97(2)−1.98(2)	C(45)−Fe(1)−C(46)	177.5(7)
N(5)−C(45)	1.12(2)	Fe(1)−C(45)−N(5)	173(2)
N(10)−C(46)	1.14(2)	Fe(1)−C(46)−N(10)	177(2)
Cu(1)−N(5)	1.89(1)	Cu(1) Center	
Cu(1)−N(6−9), range	2.00(1)−2.10(2)	Cu(1)−N(5)−C(45)	168(2)
Cu(2)−N(10)	1.92(1)	N(5)−Cu(1)−N(6)	178.0(6)
Cu(2)−N(11−14), range	2.04(2)−2.07(2)	N(7)−Cu(1)−N(8)	117.6(6)
		N(7)−Cu(1)−N(9)	114.7(6)
		N(8)−Cu(1)−N(9)	122.5(6)
		N(5)−Cu(1)−N(7−9), range	96.8(6)−98.8(7)
		N(6)−Cu(1)−N(7−9), range	81.9(6)−82.1(6)
		Cu(2) Center	
		Cu(2)−N(10)−C(46)	175(2)
		N(10)−Cu(2)−N(11)	178.4(6)
		N(12)−Cu(2)−N(13)	115.5(6)
		N(12)−Cu(2)−N(14)	119.5(7)
		N(13)−Cu(2)−N(14)	119.0(6)
		N(10)−Cu(2)−N(12−14), range	96.7(7)−99.0(6)
		N(11)−Cu(2)−N(12−14), range	80.8(7)−82.5(6)

$[(F_8$-TPP)Fe^{III}-$(CN)_2$-$\{Cu^{II}(TMPA)\}_2](PF_6)_3$ (**6**-$(PF_6)_3$) is shown in Figure 3. A summary of pertinent bond distances and angles is given in Table 2. The six-coordinate heme-iron, with two near-linear axial carbon-bound ligands (∠Fe−C−N, 173 and 177°), is "capped" on either side by trigonally coordinated [Cu(TMPA)] moieties. The [Cu(2)(TMPA)] unit is coordinated in a nearly linear fashion with respect to the cyanide−iron vector (∠Cu2−N10−C46 = 175°), while the [Cu(1)(TMPA)] unit is twisted somewhat (∠Cu1−N5−C45 = 168°; see also Scheme 2 diagram). As noted in the structure of **5**, here also, two of the TMPA pyridine rings are slotted between the phenyl rings of the porphyrin while the third one lies above the plane of another phenyl group. Both Cu1 and Cu2 maintain trigonal bipyramidal geometries (τ(Cu1) = 0.93, τ(Cu2) = 0.98). Bonding distances around both copper centers are comparable (Table 2), with values in the range 2.00−2.10 Å for $N_{amine/py}$−Cu1 and 2.04−2.07 Å for $N_{amine/py}$−Cu_2, while copper-to-cyanide nitrogen atom distances are Cu1−N5 = 1.89 Å, Cu2−N10 = 1.92 Å. Geometric information again characterizes the heme-iron as being low-spin:[31] the iron atom is located in the plane formed by the pyrrole nitrogens (displacement = 0.02 Å) and average iron−pyrrole distances of 1.98 Å are found. In contrast with related structures reported by Scheidt and Holm, the iron-to-cyanide bond distances are elongated (1.98(2) Å). For the mononuclear iron-porphyrin, (py)(TPP)Fe(CN),[34] the Fe−C_{CN} distance is 1.908 Å whereas this bond length in dinuclear μ-cyanide Fe^{III}−Cu^{II} complexes range from 1.86 to 1.92 Å.[12b,c] A similar trinuclear derivative reported by Holm[12c] (vide infra) was found to have FeC_{CN} bonds at 1.94 Å. This trend suggests that steric requirements as well as the number of bridged groups influence the bonding in these compounds.

Compounds $[(py)(F_8$-TPP)Fe^{III}-CN-$Cu^{II}(TMPA)]^{2+}$ (**5**) and $[(F_8$-TPP)Fe^{III}-$(CN)_2$-$\{Cu^{II}(TMPA)\}_2]^{3+}$(**6**) represent additions to the series of structures reported earlier by Holm and co-workers, wherein various copper(II)−ligand and (OEP)Fe(III)−B (OEP = octaethylporphyrinate; B = pyridine or

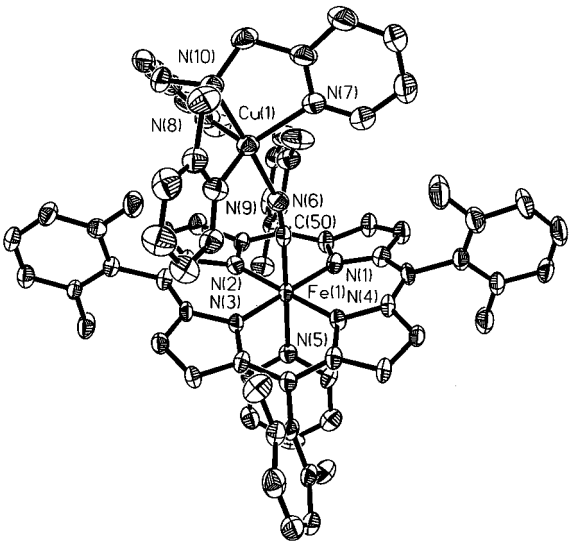

Figure 2. ORTEP view of cation [(py)(F_8-TPP)Fe^{III}-(μ-CN)-Cu^{II}-(TMPA)]$^{2+}$ (**5**).

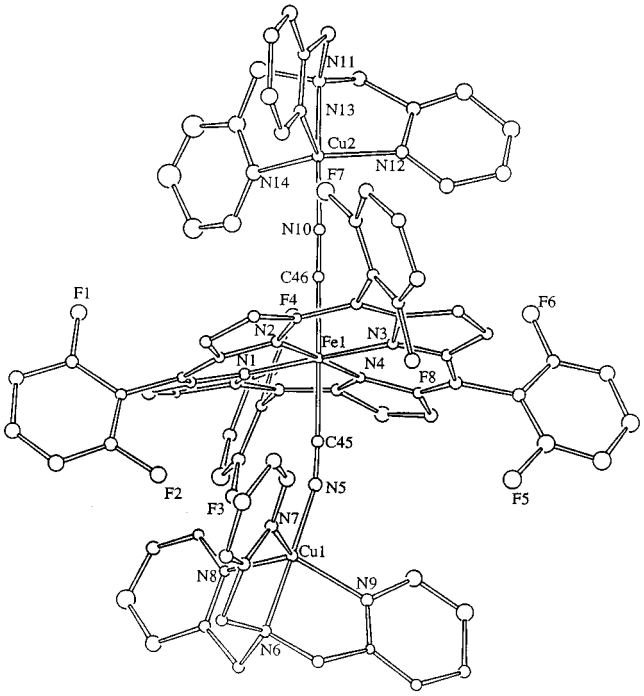

Figure 3. ORTEP view of cation [(TMPA)Cu^{II}-(μ-CN)-(F_8-TPP)Fe^{III}-(μ-CN)-Cu^{II}(TMPA)]$^{3+}$ (**6**).

1-methylimidazole) complexes form assemblies through μ-CN^- bridges.[12] In all structures, the bridging ligand is bound to copper by the N atom with Cu−N_{CN} distances ranging from 1.88(1) to 2.171(7) Å. The Fe−C_{CN}−N_{CN} angles are essentially linear throughout; however, Cu−N_{CN}−C_{CN} angles vary significantly (147.3(5)−174.5(1)°). The most comparable complex to **5** is [(py)(OEP)Fe-CN-Cu(NPy3)]$^{2+}$ (Npy3 ≡ TMPA)[12g] and hence varies only slightly except for an unexpectedly larger Cu−N_{CN}−C_{CN} angle of 174.5(8)° vs 163.8(5)° for **5**. Excluding this complex, the structure with the closest resemblance to **5** is [(py)-(OEP)Fe-CN-Cu(Me_6tren)]$^{2+}$ (Me_6tren = tris(2-(dimethylamino)-ethyl)amine).[12a,c] Here, as in **5**, a trigonal copper complex with tripodal tetradentate amine ligand is ligated through an axial cyanide bond to the porphyrin iron. The main differences are found in somewhat shorter pyrrole−iron distances (1.967_{ave} vs 2.00_{ave} Å), a longer Cu−N_{CN} distance (1.945 vs 1.88(1) Å), and notably smaller Fe−C_{CN}−N_{CN} (174.6 vs 179.1°) and Cu−N_{CN}−C_{CN} (163.8 vs 174.1°) angles for **5**. Steric requirements of the TMPA moiety may contribute to the assembly's deviation from linearity. These differences are also reflected in the CN stretching frequency observed when comparing this property in **5** to [(py)(OEP)Fe-CN-Cu(Me_6tren)]$^{2+}$ (vide infra).

The trinuclear analogue reported by Holm and co-workers is [(OEP)Fe^{III}-$(CN)_2$-{Cu^{II}(Me_6tren)}$_2$]$^{3+}$, a centrosymmetric complex wherein the bridging ligands fill the axial positions of the copper coordination sphere and are bound in a nonlinear fashion (Cu−N_{CN}−C_{CN}, 171.8(9)°, and Fe−C_{CN}−N_{CN}, 173(1)°).[12c] Complex **6**, being noncentrosymmetric is notably different with one copper fragment bound in a nearly linear fashion while the other is tilted (Cu−N_{CN}−C_{CN}, 175(2) and 168(2)°; Fe−C_{CN}−N_{CN}, 173(2) and 177(2)°). Further comparisons reveal slightly shorter Cu−N_{CN} (1.89(1), 1.92(1) vs 1.94(1) Å) and marginally longer Fe−C_{CN} (1.98(2), 1.98(2) vs 1.94(1) Å) distances for **6**.

IR Stretching Frequency. The cyanide stretching frequency of [(py)(F_8-TPP)Fe^{III}-CN-Cu^{II}(TMPA)]$^{2+}$ (**5**) was measured as 2170 cm^{-1} in the solid state (KBr). Based on their work on μ-CN^- heme-copper oxidase models, Holm and co-workers[12b−d] have noted the relationship between cyanide stretching frequency (ν_{CN}) and Cu−CN bond length and angle, wherein ν_{CN} increases with increasing Cu−N_{CN}−C_{CN} angle and decreasing Cu−NC distance, and have established with reasonable certainty the existence of the Fe^{III}−CN−Cu^{II} bridge motif in the cyanide treated oxidized enzyme. They noted that for the enzyme, ν_{CN} falls within a narrow range of 2152−2146 cm^{-1}. To date, none of the structurally characterized model compounds[12b−d] displays a ν_{CN} in this range, including now, [(py)(F_8-TPP)Fe^{III}-CN-Cu^{II}-(TMPA)]$^{2+}$ (**5**). However, the properties (i.e., structure, ν_{CN}) of **5** do agree well with relationships established for these other model systems and, as mentioned, compare closely in structure with [(py)(OEP)Fe-CN-Cu(Me_6tren)]$^{2+}$, which possesses ν_{CN} = 2177 cm^{-1}.

Thus, the structural and physical properties of the [PFe^{III}-CN-Cu(ligand)]$^{2+}$ moiety vary little with differences in P (i.e., OEP vs F_8-TPP) or tripodal tetradentate nitrogen donor ligand (i.e., tertiary amine containing Me_6tren vs pyridylamine containing TMPA).

Paramagnetically Shifted NMR Spectra of Cyano-Copper-(II) Complexes. NMR spectroscopic properties of heme proteins or synthetic iron-porphyrins, including paramagnetic systems (i.e., all except low-spin iron(II)), have been and continue to be of considerable interest.[38] While mononuclear iron(III)−porphyrin complexes do exhibit shifted but readily observable ^{1}H NMR spectroscopic resonances, the long electronic relaxation time (τ_s 10^{-9} s) for typical mononuclear Cu(II) complexes normally precludes ^{1}H NMR signal observation. However, magnetic coupling of a copper(II) complex to another paramagnet such as copper(II),[21] or iron(III), as in μ-O^{2-} or μ-OH^- complexes [(F_8-TPP)Fe^{III}-O(H)-Cu^{II}(TMPA)]$^{+/(2+)}$, allows observation of upfield shifted TMPA resonances (e.g., to −105 ppm), due to the S = 2 electronic ground state.[17] With the current interest in NMR properties of coupled systems,[17,18,21] we have also studied the cyano-copper(II) containing compounds described in this report.

(38) (a) Walker, F. A.; Simonis, U. In *Biological Magnetic Resonance, Vol. 12, NMR of Paramagnetic Molecules*; Berliner, L. J., Reuben, J., Eds.; Plenum Press: New York, 1993; pp 133−274. (b) Satterlee, J. D.; Alam, S.; Yi, Q.; Erman, J. E.; Constantinidis, I.; Russell, D. J.; Moench, S. J. In *Biological Magnetic Resonance, Vol. 12, NMR of Paramagnetic Molecules*; Berliner, L. J., Reuben, J., Eds.; Plenum Press: New York, 1993; pp 275−298. (c) Banci, L.; Bertini, I.; Luchinat, C.; Pierattelli, R.; Shikhirev, N. V.; Walker, F. A. *J. Am. Chem. Soc.* **1998**, *120*, 8472−8479.

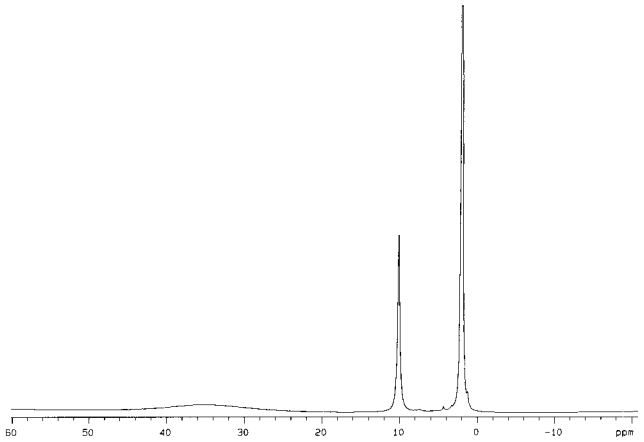

Figure 4. ^{1}H NMR spectrum of $[Cu^{II}(TMPA)(CN)]^+$ (**2**) in CD_3CN.

^{1}H NMR Spectra of $[Cu(TMPA)(CN)]^+$ (2) and $[(F_8\text{-TPP})Fe(py)(CN)]$ (3). Despite the usual difficulty with line-broadening in ^{1}H NMR spectra of mononuclear copper(II) complexes, we were previously able to obtain the paramagnetically shifted spectrum of $[Cu(TMPA)(CH_3CN)]^{2+}$ and assign the signals by preparing the methylated ligand analogues (n-Me)$_3$-TMPA (n = 3, 4, and 5).[17] It was shown that the 3- and 5-pyridyl protons resonate at approximately the same position in the spectrum (as a broad peak at 30 ppm) while the most distant pyridyl 4-H is found to give a peak at 10.5 ppm.[17] When comparing the spectrum of $[Cu^{II}(TMPA)(CH_3CN)]^{2+}$ with $[Cu^{II}(TMPA)(CN)]^+$ (**2**) (Figure 4), once again we see the pyridyl-3 and -5 proton signals together at 35 ppm and the pyridyl 4-H at 10.1 ppm. As was noted for $[Cu^{II}(TMPA)(CH_3CN)]^{2+}$, this reduction of the chemical shift as a function of the relative distance from the paramagnetic metal center is indicative of a σ contact shift mechanism.[17] For this reason, the methylene protons and the pyridyl-6 proton eluded detection.

The ^{1}H NMR spectrum (not shown) of the synthon compound $[(F_8\text{-TPP})Fe(py)(CN)]$ (**3**) is indicative of its low-spin nature. The *meta*- (split at 7.99 and 7.70 ppm) and *para*-phenyl (7.30 ppm) signals are upfield shifted compared to that seen for high-spin iron(III) compounds.[14a] The more diagnostic feature is the pyrrole resonance, found at −19.6 ppm, which is a typical low-spin position.[31] After the pyrrole-deuterated version of **3** was prepared, starting from its μ-oxo dimer, this latter signal was unequivocally assigned to this position using ^{2}H NMR spectroscopy. Likewise, when the preparation of **3** was carried out using pyridine-d_6 as one of the reactants, ^{2}H NMR spectroscopy established that the peaks at 18.3, 10.1, 6.3, 5.7, and 1.6 ppm (spectrum not shown) as resulting from the axial base. We note the unusual nature of observing five separate pyridine signals in this complex. Apparently, all pyridine protons in this complex are chemically inequivalent on the NMR time scale, possibly due to slow rotation and the presence of axial ligand orientational effects (i.e., preferred conformation).[38a,39] Ligand binding "pockets" and hence hindered rotation of axial ligands have been reported for bis-imidizole and -pyridine Fe(III)-porphyrin complexes which have ruffled porphyrin rings.[39a,c]

NMR Spectroscopic Assignments for $[(py)(F_8\text{-TPP})Fe^{III}\text{-CN-}Cu^{II}(TMPA)]^{2+}$ (5) and $[(F_8\text{-TPP})Fe^{III}\text{-}(CN)_2\text{-}\{Cu^{II}(TMPA)\}_2]^{3+}$ (6). ^{1}H NMR spectra signals for compounds **5** and **6** are provided in Figure 5, and assignments for **5** are given in Figure 6 and Table 3. The complete assignment was achieved by employing a stepwise deuteration and/or methylation of TMPA and porphyrinate pyrrole/pyridine positions. This involved preparation of starting materials that were methylated (for TMPA) or deuterated (TMPA and porphyrin) on selected positions, followed by complexation with copper or iron and construction of the desired di- or trinuclear structure using these methylated or deuterated synthons. Comparison of the ^{1}H NMR spectra of these compounds with those of "authentic" **5** and **6** allowed for the assignment of the various signals. The spectra

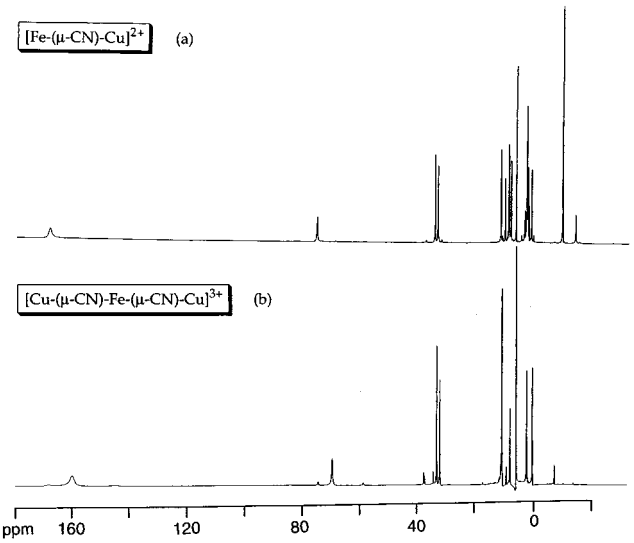

Figure 5. ^{1}H NMR spectra (CD_2Cl_2) and comparisons of (a) $[(py)(F_8\text{-TPP})Fe^{III}\text{-}(\mu\text{-CN})\text{-}Cu^{II}(TMPA)]^{2+}$ (**5**) and (b) $[(TMPA)Cu^{II}\text{-}(\mu\text{-CN})(F_8\text{-TPP})Fe^{III}\text{-}(\mu\text{-CN})\text{-}Cu^{II}(TMPA)]^{3+}$ (**6**).

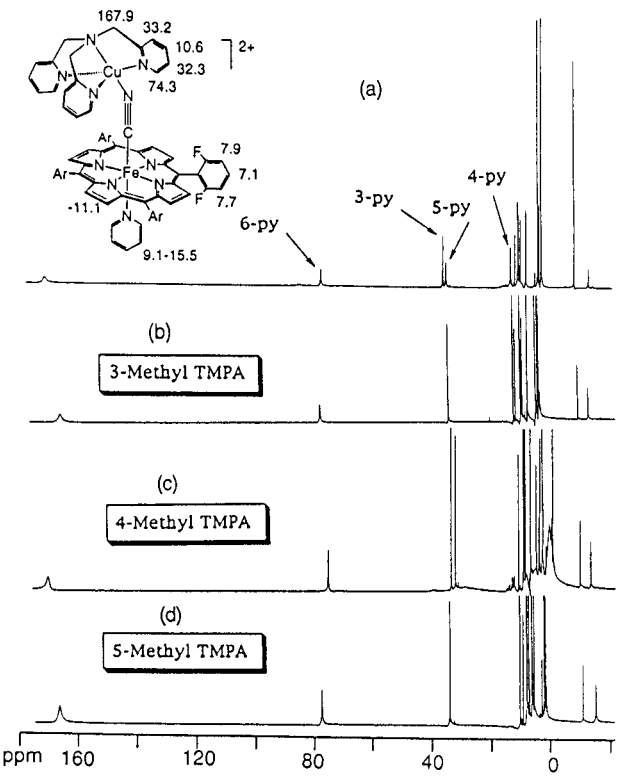

Figure 6. NMR spectra (CD_2Cl_2) of (a) $[(py)(F_8\text{-TPP})Fe^{III}\text{-}(\mu\text{-CN})\text{-}Cu^{II}(TMPA)]^{2+}$ (**5**), (b) $[(py)(F_8\text{-TPP})Fe^{III}\text{-}(\mu\text{-CN})\text{-}Cu^{II}((3\text{-Me})_3\text{-TMPA})]^{2+}$, (c) $[(py)(F_8\text{-TPP})Fe^{III}\text{-}(\mu\text{-CN})\text{-}Cu^{II}((4\text{-Me})_3\text{-TMPA})]^{2+}$, and (d) $[(py)(F_8\text{-TPP})Fe^{III}\text{-}(\mu\text{-CN})\text{-}Cu^{II}((5\text{-Me})_3\text{-TMPA})]^{2+}$.

(39) (a) Nakamura, M.; Ikeue, T.; Fujii, H.; Yoshimura, T.; Tajima, K. *Inorg. Chem.* **1998**, *37*, 2405−2414. (b) Safo, M. K.; Nesset, M. J. M.; Walker, F. A.; Debrunner, P. G.; Scheidt, W. R. *J. Am. Chem. Soc.* **1997**, *119*, 9438−9448. (c) Safo, M. K.; Gupta, G. V.; Watson, C. T.; Simonis, U.; Walker, F. A.; Scheidt, W. R. *J. Am. Chem. Soc.* **1992**, *114*, 7066−7075.

Table 3. Comparison of the Chemical Shifts (ppm) in ^{1}H NMR Spectra of [(py)(F_8-TPP)Fe^{III}-(μ-CN)-Cu^{II}(TMPA)](ClO_4)$_2$ (**5**) with Deuterated and Methylated Analogs in CD_2Cl_2 at 298 K

5	pyrrole-d_8 F_8-TPP	pyridine-d_5 F_8-TPP	methylene-d_6 TMPA	(3-Me)$_3$-TMPA	(4-Me)$_3$-TMPA	(5-Me)$_3$-TMPA	assignment
167.9	167.4	168.0		163.3	168.8	166.0	methylene TMPA
74.3	74.2	75.0	75.2	76.0	74.2	77.8	(6-pyridyl H TMPA)
33.2	33.1	33.5	33.5		32.5	34.2	3-pyridyl TMPA
32.3	32.2	32.5	32.6	32.4	31.0		5-pyridyl TMPA
10.6	10.6	10.9	10.6	10.3		10.2	4-pyridyl TMPA
9.1	9.2		9.2	9.5	9.5	9.1	pyridine
7.9	7.9	7.9	7.9	7.8	7.9	7.9	(*meta*-phenyl)
7.7	7.7	7.7	7.7	7.6	7.6	7.7	(*meta*-phenyl)
7.1	7.1	7.1	7.1	7.1	7.1	7.1	(*para*-phenyl)
						6.1	5-Me TMPA
				2.7			3-Me TMPA
					−2.3		4-Me TMPA
−11.1		−11.3	−11.4	−11.7	−11.7	−11.4	pyrrole
−15.5	−15.5		−15.8	−15.3	−15.4	−15.8	pyridine

of the derivatives of both ligands and complexes, apart from the expected changes, were invariant with respect to their parent spectra, indicating the formation of essentially identical structures, thus permitting a direct comparison and assignment of the signals.

The ^{1}H NMR spectrum of [(py)(F_8-TPP)Fe^{III}-CN-Cu^{II}-(TMPA)]$^{2+}$ (**5**) is highly featured and encompasses the region from +168 to −16 ppm (Figure 5a). As described above, incorporating a deuterium label in the various starting compounds allowed for the assignment of different signals. In this manner, the resonance at −11.1 ppm was assigned to the pyrrole protons, and the signals at 9.1 and −15.5 ppm to the pyridine axial base. Furthermore, deuterium NMR identified three more broad signals arising from the pyridine base (at 13.6, 2.6, and −12.0 ppm) that go undetected in the ^{1}H NMR spectrum. The most downfield-shifted peak at 167.9 pm is assigned to the methylene groups of the TMPA ligand on copper; the low intensity suggests the possibility that this signal may be due to only one of two protons present in a given methylene group, the other being unobserved. The porphyrin *m*- and *p*-phenyl resonances are observed at 7.9, 7.7, and 7.1 ppm (assignments based on 2-D COSY experiment), respectively. The remaining signals were assigned by using methylated TMPA analogues. As we noted above, comparison of the spectra of [(F_8-TPP)-Fe-CN-Cu((*n*-Me)$_3$-TMPA)]$^{2+}$ with **5** clearly shows which methyl substituent corresponds to the proton it replaces on the TMPA ligand; this signal will no longer be present while the rest of the pyridyl positions remain essentially unchanged (Figure 6). Having prepared the corresponding 3-, 4-, and 5-methylated versions of **5**, the following assignments could be made: 33.2 ppm (3-pyridyl), 32.3 (5-pyridyl), and 10.6 ppm (4-pyridyl) (see Figure 6 and Table 3). This leaves the unassigned signal at 74.3 ppm which we tentatively ascribed to the TMPA pyridyl-6 proton. A ^{19}F NMR spectrum of **5** (not shown) reveals a split signal for the *o*-fluorine atoms on the phenyl rings at 114 and 115 ppm upfield from $CFCl_3$. This observation strongly suggests retention of the structure as determined by X-ray crystallography and is in line with the observation of split *m*-phenyl protons in the ^{1}H NMR spectrum. Furthermore, there is no evidence of dissociation (*ie.* signals of mononuclear species) in solution.

The ^{1}H NMR spectrum of the trinuclear complex [(F_8-TPP)-Fe^{III}-(CN)$_2$-{Cu^{II}(TMPA)}$_2$]$^{3+}$ (**6**) bears a close resemblance to that of binuclear complex **5**. It essentially spans the same region (158 to − 8 ppm) and the same peak pattern is found (Figure 5b). Major differences include the lack of pyridine axial base signals (as expected) and a slight downfield shift in the pyrrole signal (from −11.1 to −8 ppm). The latter signal was assigned on the bases of deuteration and the remaining by comparison to the binuclear complex **5**.

As was invoked for [Cu^{II}(TMPA)(CN)]$^+$ (**2**), ^{1}H NMR spectra of both **5** and **6** suggest that a σ contact shift mechanism is operative. Here, too, replacement of the 3- and 5-pyridyl protons of TMPA by a methyl group does not alter the sign of the shifts (δ = 2.7 and 6.1 ppm, respectively), as would have been expected for a π contact shift mechanism, but merely its magnitude. The relative *upfield* shift of the 4-Me TMPA signal (δ = −2.7 ppm) may be explained by the additional bond between the metal center and this position which gives rise to a diminished σ contribution to the contact shift. Based on comparison with the natural enzyme[3a,40] and the very closely structurally related well-characterized (i.e., by Mössbauer spectroscopy) model compound discussed, i.e., [(py)(OEP)Fe-CN-(Me$_6$tren)]$^{2+}$,[12a−c] it is reasonable to conclude that **5** similarly possesses ferromagnetically coupled low-spin Fe^{III} (S = $^1/_2$) and Cu^{II} (S = $^1/_2$) ions, giving rise to an S = 1 ground-state spin system (with S = 0 excited state). The room-temperature magnetic moment (μ_{eff} = 2.7 μ_B) and NMR properties are also consistent with this conclusion. On the basis of work carried out by Bertini, Luchinat, and co-workers, we can deduce the sign of the hyperfine shift from eq 3:[18]

$$\Delta\nu/\nu_0 = (2\pi g_e \mu_B/3h\gamma_N kT)\sum A_i\langle S_{iZ}\rangle \qquad (3)$$

All symbols have their usual meaning; S_{iZ} is the expectation value evaluated over all S_i states (S = 1 and 0) and averaged according to multiplicity ($2S_i$ + 1) and Boltzmann population. The isotropic hyperfine coupling constant between a ligand hydrogen nucleus and spin state S_i (S = 1 or 0) for both metals is given by A_i. When assuming that a hydrogen nucleus on the TMPA ligand interacts with only one metal (e.g. Cu), the relationship between the hyperfine coupling constant A_{Cu} and A_i is given by

$$A_i = A_{Cu}C_{iCu} \qquad (4)$$

In this equation C_{iCu} is a coefficient which represents a scaling of the hyperfine coupling constant A_{Cu}. Based on the tabulations reported by Luchinat and Ciurli,[18b] the coefficient associated with the S = 1 (ground state) for a ferromagnetically coupled S = $^1/_2$ (Fe) and S = $^1/_2$ (Cu) system is $^1/_2$, for interaction of a hydrogen nucleus with the Cu ion. The sign of the coefficient

(40) Kent, T. A.; Münck, E.; Dunham, W. R.; Filter, W. F.; Findling, K. L.; Yoshida, T.; Fee, J. A. *J. Biol. Chem.* **1982**, *257*, 12489.

is in line with what is observed in the ^{1}H NMR spectrum, *i.e.*, *downfield*-shifted signals for protons sensing Cu.

In previous work, we have used this equation to infer the sign of shifts of hydrogen nuclei sensing Cu in [(F_8-TPP)Fe^{III}-O-Cu^{II}(TMPA)]$^+$, an antiferromagnetically coupled Fe ($S = {}^5/_2$)−Cu ($S = {}^1/_2$) system.[17] The coefficients for Cu in the ground state ($S = 2$) are negative ($-{}^1/_6$) and in agreement with the observed *upfield*-shifted TMPA (Cu−ligand) proton signals. The present case shows the other extreme of magnetically induced isotropic shift possibilities for an iron−copper coupled system.

In theory, coupling between two paramagnetic metal ions may alter their electronic relaxation times. In the case of two different metal ions, the one having the shorter τ_s (electronic relaxation time) facilitates an additional relaxation pathway for the slower relaxing metal, resulting in a smaller τ_s. For our system, the electronic relaxation times for low-spin iron(III) are in the order of 10^{-11}−10^{-12} s, while that for copper(II) is approximately 10^{-9} s.[18b] Scalar coupling between the two metal sites results in enhanced relaxation of Cu(II), giving rise to the observation of sharper proton signals of the Cu(II) ligand relative to the uncoupled, mononuclear complex [Cu^{II}(TMPA)(CN)]$^+$ (**2**).

As mentioned before, the solution NMR properties of trinuclear complex [(F_8-TPP)Fe^{III}-$(CN)_2$-{Cu^{II}(TMPA)}$_2$]$^{3+}$ (**6**) are comparable to those observed for **5**. Although there is the potential for a more complicated spin system ($S = {}^1/_2$ Cu(II) − $S = {}^1/_2$ LS Fe(III) − $S = {}^1/_2$ Cu(II)), we conjecture that the similarity of ^{1}H NMR properties of **6** to those of **5**, suggest that **6** may be behaving like a species with one essentially independent ferromagnetically coupled $S = {}^1/_2$ Cu(II) − $S = {}^1/_2$ Fe(III) unit ($S = 1$ system, like in **5**), together summed with the other $S = {}^1/_2$ Cu(II) moiety. In fact, the measured solution magnetic moment ($\mu_{eff} = 3.4\ \mu_B$) for **6** is lower than would be expected for an $S = {}^3/_2$ system (expected $\mu_{eff} = 3.9\ \mu_B$), and in the range reasonable for an {$S = 1$ plus $S = {}^1/_2$} system (expected $\mu_{eff} = 3.3\ \mu_B$). The absence of any ^{1}H NMR signals arising from mononuclear [Cu^{II}(TMPA)(CN)]$^+$ is noted. Lower intensity signals are seen in the vicinity of the major TMPA signals. It is speculated that these could be the result of dynamic behavior of the TMPA moieties which is slow on the NMR time scale. Further studies on **6**, such as the investigation of the temperature dependence of the NMR signals,[18,38] would be needed to fully understand its magnetic and electronic properties.

Conclusion

We have shown the feasibility of generating both binuclear and trinuclear cyanide-bridged iron(III)−copper(II) complexes, [(py)(F_8-TPP)Fe^{III}-CN-Cu^{II}(TMPA)]$^{2+}$ (**5**) and [(F_8-TPP)Fe^{III}-$(CN)_2$-{Cu^{II}(TMPA)}$_2$]$^{3+}$ (**6**), utilizing a porphyrin and copper-ligand not previously used for these types of compounds. Close inspection of starting synthons verifies an important feature in the control of formation of either a monosubstituted or disubstituted porphyrin product, viz. the presence or absence of an axial base (here, pyridine), respectively.

The complexes have been characterized in some detail, in particular by X-ray crystallography and ^{1}H and ^{2}H NMR spectroscopy. Structural analysis indicates a low-spin iron(III) porphyrin bridging through cyanide to copper(II)(TMPA) moiety in **5**. Assignments of NMR signals have been made following methylation or deuteration of selected positions in the starting synthons. Spectroscopic data supports the retention of the iron low-spin state in solution as indicated by the upfield shifted pyrrole resonance. The NMR and magnetic data suggest both **5** and **6** display some degree of ferromagnetic coupling between Cu(II) and low-spin Fe(III). This helps to explain the enhancement of the electronic relaxation rate for Cu(II) which entails sharp proton NMR signals of the Cu(TMPA) moiety and the large downfield shifts of the TMPA hydrogens. The present work provides an additional example of the relationship between the ^{1}H NMR spectroscopic profiles and the magnetic/electronic properties of heme-copper complexes.

Future work will focus on the synthesis and characterization of additional and other types of Fe^{III}-X-Cu^{II} bridged species.

Acknowledgment. We thank the National Institutes of Health (GM28962) for support of this research and the Delft University of Technology for support for DMC.

Supporting Information Available: Tables and figures, with full details of the X-ray structural analysis and data for complexes **2**, **5**, and **6**, and fully labeled structure diagrams for **5** and **6**. This material is available free of charge via the Internet at http://pubs.acs.org.

IC981091S